J Solid State Electrochem (2011) 15:183–188
DOI 10.1007/s10008-010-1084-y

ORIGINAL PAPER

Platelike CoO/carbon nanofiber composite electrode with improved electrochemical performance for lithium ion batteries

Wenli Yao · Jinqing Chen · Hongwei Cheng

Received: 22 November 2009 / Revised: 21 April 2010 / Accepted: 23 April 2010 / Published online: 15 May 2010

Abstract Platelike CoO/carbon nanofiber (CNF) composite materials with porous structures are synthesized from the thermal decomposition and recrystallization of β-$Co(OH)_2$/CNF precursor without the need for a template or structure-directing agent. As negative electrode materials for lithium-ion batteries, the platelike CoO/CNF composite delivers a high reversible capacity of 700 mAh g^{-1} for a life extending over hundreds of cycles at a constant current density of 200 mA g^{-1}. More importantly, the composite electrode shows significantly improved rate capability and electrochemical reversibility. Even at a current of 2 C, the platelike CoO/CNF composite maintain a capacity of 580 mAh g^{-1} after 50 discharge/charge cycles. The improved cycling stability and rate capability of the CoO/CNF composite electrodes may be attributed to synergistic effect of the porous structural stability and improved conductivity through CNF connection.

Keywords Cobalt oxide · Carbon nanofiber · Composite material · Anode · Lithium-ion batteries

Introduction

Designing electrode materials with high lithium storage capacity, rate capability, and long cycling life are still the major challenges for developing high performance lithium-ion batteries (LIBs). As the most widely used anodes, conventional graphite-based anode materials exhibit excellent charge and discharge cycling performance, yet their capacity for lithium storage is limited to less than 372 mAh g^{-1} [1]. More recently, the rapid development of high-power LIBs has been requested to meet the growing demand for use in portable electronic devices and hybrid electric vehicles. Thus, various new high-performance anode materials have been intensively investigated for next-generation LIBs [2–5]. Among the various sorts of transition metal oxides, cobalt oxides (CoO, Co_3O_4) are attractive due to the high Li-storage capacities about three times larger than those of graphite [2, 6–8]. However, despite their ultrahigh capacity, these cobalt oxides still suffer from large initial irreversible loss, low capacity retention upon cycling, and poor rate capability, due to the poor electronic conductivity and large volume changes during repeated lithiation/delithiation reactions [7–10].

For the powder materials of cobalt oxides, CoO particles can usually present much better charge and discharge performance than the Co_3O_4 particles [2, 9, 11, 12]. Furthermore, due to about three times the capacity of commercial graphite anode, Co_3O_4 powder materials have been intensively investigated and their rate capability has been also improved by preparing mesoporous Co_3O_4 nanowire [13] or macroporous platelet-like Co_3O_4 anodes [14]. The porosity of electrode materials allows for easy diffusion of electrolyte into the inner region of the electrode, resulting in large electrode-electrolyte contact area for Faradaic reactions, reduced internal resistance, and improved high-power performance [13–15]. As an example, mesoporous Co_3O_4 nanowire arrays had showed large reversible capacity, good cycleability, and high-rate capability. The mesoporous NW arrays on Ti substrate can

W. Yao · H. Cheng
Shanghai Key Laboratory of Modern Metallurgy and Materials Processing, Shanghai University,
149 Yanchang Road,
Shanghai 200072, China

W. Yao (✉) · J. Chen
Jiangxi Research Institute of Tungsten and Rare Earths,
Ganzhou 341000, China
e-mail: wenliyao@shu.edu.cn

maintain a stable capacity of 700 mAh g^{-1} at a current of 1 C after 20 cycles [13]. Therefore, the electrode materials with porous structure on conducting substrate will hold promise for developing high performance LIBs. Compared with Co_3O_4 powder materials, there are very few reports on the improvements of rate capability of CoO powder materials.

It has been revealed that the electrochemical lithiation of CoO leads to the formation of Li_2O and nanodispersed metallic Co, along with the formation of the solid electrolyte interphase (SEI) layer [16–18]. Surface analysis of the formed CoO anode revealed that the SEI contains various organic and inorganic electrolyte reduction/decomposition products, which may result in large irreversible capacity during the first discharging process [17, 18]. Meanwhile, an effective SEI film is supposed to protect the electrode by separating the cobalt active material from side reactions and to allow a stable lithium insertion/extraction process. Owing to high specific capacity, low electrode potential, long cycle life and a high level of safety, several types of carbon nanofibers (CNFs) have been successfully used in lithium battery applications [19–21]. Furthermore, CNF anode materials can also form high-quality SEI film and exhibit high reversible capacity and high rate capability due to nanometer-sized diameters (fast Li^+ diffusion path) and relatively good electrical conductivity [22, 23]. The conducting connections will be improved when CNFs are used in the anode preparation. In the present study, we report the porous platelike CoO/CNF composite anode with improved rate capability and excellent reversible capacity.

Experimental

All reaction reagents are analytic grade reagents and directly used without further treatment. The commercial carbon nanofiber with average diameter of 200 nm was ultrasonically dispersed in an 18.5 wt% HCl solution at 30 °C for 5 h, intensively washed with deionized water and dried in vacuum. In a typical reaction, 2.2 g of $Co(NO_3)_2{\cdot}6H_2O$ were dissolved into 100 ml of isopropyl alcohol-water (1:1, *v*/*v*) solution in a three-necked round bottom. Of the acid-treated CNF, 0.2 g was dispersed in the above solution by ultrasonication for 30 min. Then, appropriate amount of ammonia-isopropyl alcohol solution was added into the suspending solution and aged for 10 min to form the Co$(OH)_2$/CNF gel at room temperature. The $Co(OH)_2$/CNF gel precursor was then transferred into a Teflon-lined autoclave with 75-80% filling ratio in argon and hydrothermally treated at 120 °C for 18 h without agitation. After the autoclave was cooled down to room temperature, the β-Co$(OH)_2$/CNF product can be obtained by filtering and drying under vacuum at 70 °C. The corresponding CoO/CNF composites were finally obtained by calcining the β-Co$(OH)_2$/CNF precursor at 550 °C in Ar flow for 2 h. Assumed that there was no weight loss of CNF during filtering and pyrolysis, the weight ratio for CNF means the original CNF weight (0.2 g) divided by the final total weight of the CoO/CNF composites. In this study, the CNF content in the CoO/CNF composites with an excellent electrochemical performance was 25.1 wt%. The resulting CoO platelets were prepared by the same procedures as mentioned above but without adding CNFs.

The corresponding samples were analyzed by X-ray diffraction on a Rigaku diffractometer D/MAX-2200/PC at a scanning rate of 5° min^{-1} with a 2θ ranging from 10 to 80°, using Cu Kα radiation (1.5406 Å). Morphology of the resulting samples was observed by a JEOL field-emission microscope (JSM-7401F). Specific surface area was measured by gas adsorption on ASAP 2010 M+C (Micromeritics Inc. USA).

Electrodes consisted of 80 wt% CoO composite material, 10 wt% polyvinylidene fluoride binder, and 10 wt% acetylene black. After being blended in N-methyl-2-pyrrolidinone, the slurry was coated on a copper foil and drying under vacuum at 120 °C over 3 h. A typical electrode disk contained active material of 1.5-2.0 mg cm^{-1}. Electrochemical performance of the composite materials was evaluated using CR2016 coin cells assembled with lithium metal counter electrode, Celgard 2700 membrane separator, and electrolyte with 1 M $LiPF_6$ dissolved in the mixture of ethylene carbonate and dimethyl carbonate (1:1, *v*/*v*) in an argon-filled dry box. Cyclic voltammograms (CVs) were recorded on a CHI650C potentiostat at a scan rate of 0.2 mV S^{-1}. Galvanostatic charge (delithiation) and discharge (lithiation) was cycled between 3 and 0.01 V versus Li^+/Li on LAND CT2001A cycler at 25 °C.

Results and discussion

The phase purity and crystallinity of resulting $Co(OH)_2$/CNF and CoO/CNF composites were characterized using XRD. Figure 1a shows the XRD pattern of as-prepared Co$(OH)_2$/CNF products. Except the diffraction peaks (marked with asterisks) for carbon nanofiber, all diffraction peaks in this pattern are in good agreement with the standard Joint committee on Powder Diffraction Standards (JCPDS) card no. 30-0443. The product is confirmed to be a well-crystalline brucite-like β-$Co(OH)_2$ phase and no impurity phases are found. The corresponding XRD pattern of CoO/CNF samples is shown in Fig. 1b. All the cobalt oxide diffraction peaks at (111), (200), and (220) can be indexed as the cubic symmetry of CoO phase (space group Fm3m, JCPDS card no. 48-1719). No peaks related to β-$Co(OH)_2$ phase are observed from platelike CoO/CNF composites,

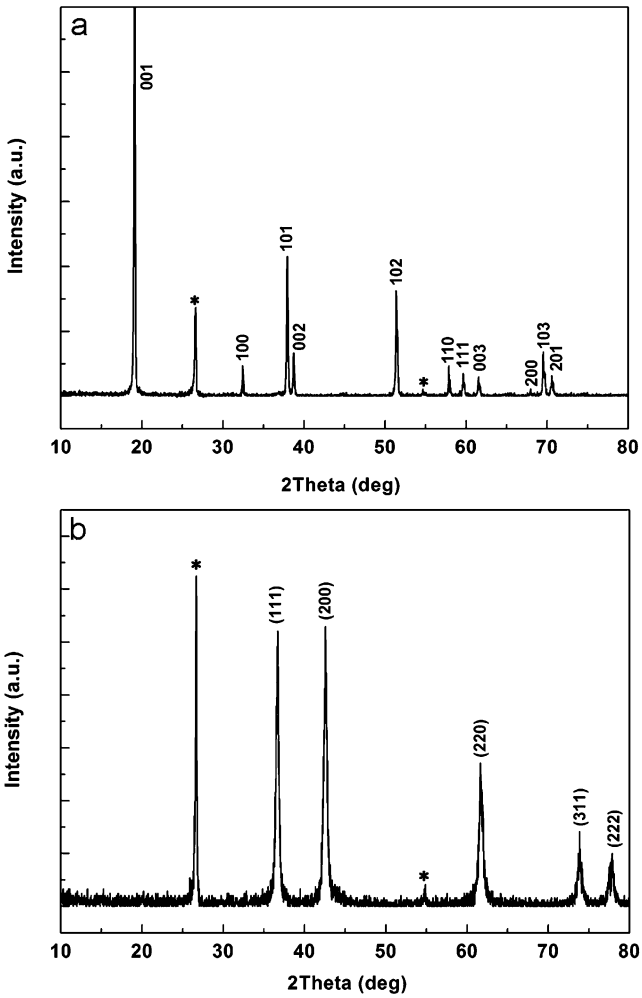

Fig. 1 XRD patterns of the resulting samples: **a** β-$Co(OH)_2$/CNF composites and **b** CoO/CNF composites. *Asterisks* response from CNF

indicating the complete decomposition of hydroxides under the corresponding experimental conditions.

Figure 2 exhibits SEM images of platelike CoO/CNF composites. The CNF has the fiber diameters with an average value of 200 nm and the lengths ranging from several to tens of micrometers. The corresponding SEM images of the obtained CoO samples shown in Fig. 2b indicate layered platelike structure with mainly average tubular size of 8 μm in diameter and 2 μm thick. For CoO/CNF composites, platelike CoO samples are evenly dispersed among CNFs and interlace CNF together to form a closely connected network via entangled CNF. And the electron conducting on the interface between electrode materials and current collector (Cu foil) can be improved effectively when CNFs act as a conducting bridge. The individual CoO platelet showed in Fig. 2c, d reveals that irregular pore distribution with the size range of 20-100 nm on its surface. However, the nanopores cannot be seen directly from the SEM images due to their small sizes, and hence other techniques are needed to evaluate the pore structure in these composites.

To further investigate the porous structure of CoO platelets clearly, the representative N_2 absorption/desorption isotherms are shown in Fig. 3. The corresponding BJH (Barret-Joyner-Halenda) pore size distribution curves (inset) reveal the porosity of CNF and CoO platelets. The pores for the CNF almost all fall into the size range of 2-4 nm. But the CoO/CNF composites exhibit obvious pore distribution with pore sizes of about 20-50 nm range with average mesopore sizes of about 30 nm, which is in agreement with the results of SEM analysis. The formation of these mesopores may be attributed to the intrinsic crystal contraction and gas evolution during the thermal decomposition reaction from $Co(OH)_2$ platelets. BET surface areas of the CNF are 16.36 $m^2\ g^{-1}$ and the specific surface areas of CoO/CNF composites are 14.84 $m^2\ g^{-1}$. Assumed that there is no change for the specific surface areas of CNF during pyrolysis, the specific surface areas of CoO are 14.32 $m^2\ g^{-1}$, which can be calculated according to the difference between the surface areas of CoO/CNF composites (14.84 $m^2\ g^{-1}$) and the absolute value of surface areas for CNF (25.1%× 16.36 $m^2\ g^{-1}$) divided by the weight percentage of CoO in the CoO/CNF composites (74.9%). Obviously, the CNF-conducting and porous-structured CoO composites will be conducive to potential electrochemical applications.

To evaluate the electrochemical performance of the CoO/CNF composite electrode, cyclic voltammograms were recorded at 25 °C in Fig. 4. In the first cycle, a small cathodic current peak appears at 0.80 V and followed by a quite large one at 0.60 V. The small cathodic peak relates to the reduction (lithiation) of CoO. And the large cathodic peak at 0.60 V corresponds to the formation of an SEI layer which is produced below 0.8 V [6, 8, 24]. Only one anodic peak at 2.08 V is found upon cycling, which can be attributed to the reaction between Co and Li_2O. By closing to 0 V, another small cathodic peak emerges. It is related to lithium insertion into CNF. During the following anodic polarization, the first peak appears at ca. 0.25 V, corresponding to lithium extraction from CNF. Compared to the first cycle, the lithiation peak at 0.80 V is shifted to 1.21 V in the second cycle. The possible reason for that the reduction peak at 0.8 V in the first cycle shifted to 1.21 V in the following cycles can be explained as follows. The newly formed Li_2O, Co products and reproduced CoO phase should be completely amorphous after the first lithiation process [2, 6, 24]. In general, an amorphous insertion phase will lose the voltage plateau character for lithium insertion and extraction, which is different from the initial crystalline CoO [6, 17, 18, 24]. Similar CVs results related to nanosized CoO electrodes were also observed by Wang et al. [9] and Do et al. [25]. The disappearance of the large cathodic peak at 0.60 V in the second cycle indicates

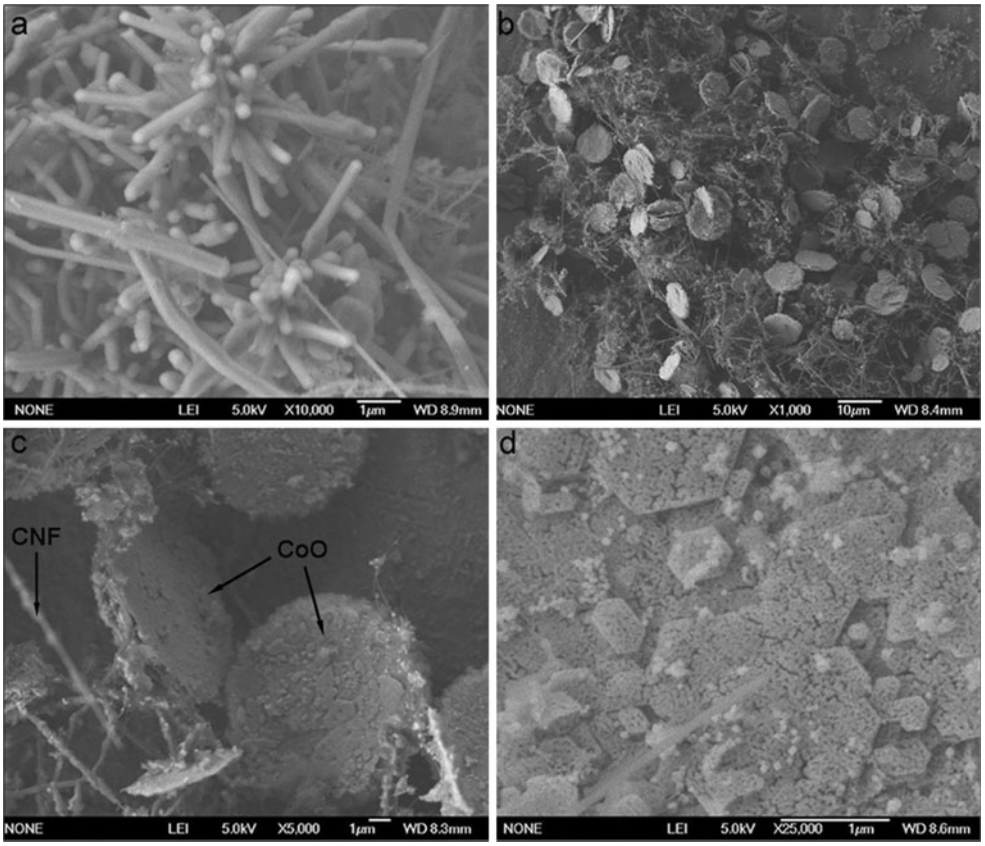

Fig. 2 SEM images of the resulting samples: **a** acid-treated CNF, **b** CoO/CNF composites, **c** high-magnification one for CoO/CNF composites, and **d** individual CoO platelet

that a complete solid electrolyte interphase film can be formed on the electrode surface after the first cycle, confirming almost no irreversible lithium loss for the SEI film during the following cycles. After the electrode activation via the 1st cycle, the well overlapped trend of the second, third, and fourth cycles show very good reproducibility and stability after the initial cycle.

Figure 5a show the first, second, 50th, and 100th charge and discharge curves of platelike CoO/CNF composite electrodes at a current density of 200 mA g^{-1} (equivalent to l Li per formula unit in 1.8 h). The voltage trends are well indicative of typical characteristics of CoO [2, 6, 8], namely, a long lithiation voltage plateau at about 0.8 V followed by a sloping curve down to the cut-off voltage of 0.01 V during the first discharge step, which is well consistent with the result of CVs. In general, the voltage hysteresis of discharging and charging profile is mainly due to the internal polarization processes of lithium conversion

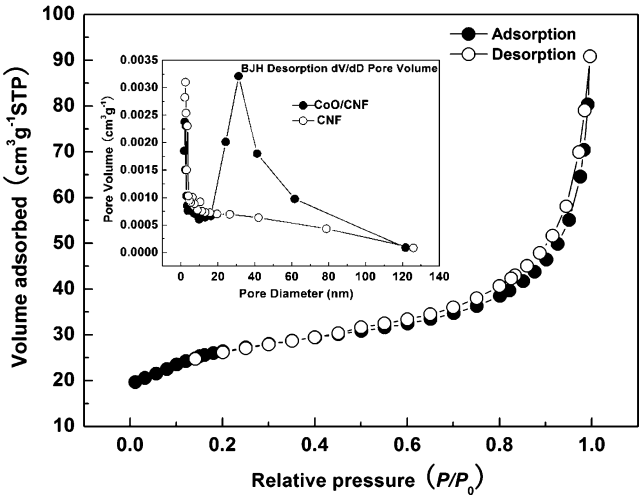

Fig. 3 N_2 adsorption/desorption isotherm and BJH pore size distributions of CoO/CNF composites

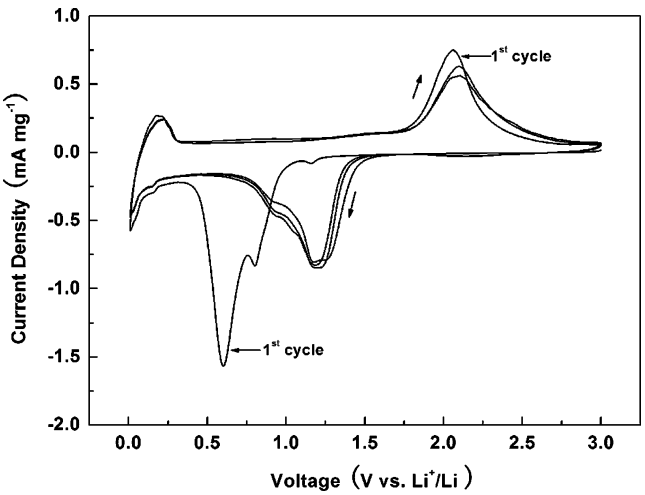

Fig. 4 Cyclic voltammograms for CoO/CNF composites at a scan rate of 0.2 mV/s

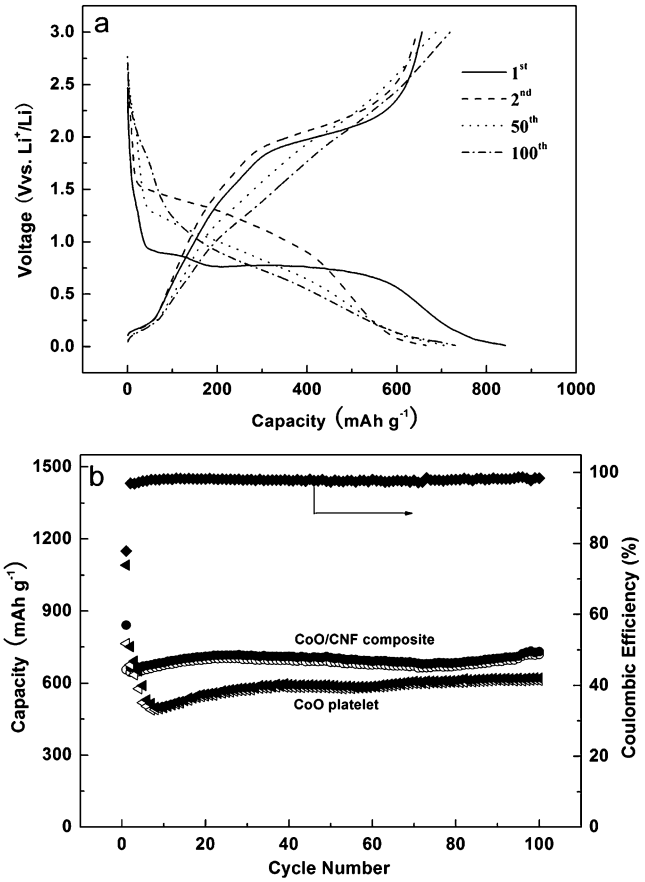

Fig. 5 **a** Charge and discharge profiles of CoO/CNF composites, **b** capacity-cycle number curve and coulombic efficiency for CoO/CNF composites and capacity-cycle number curve of CoO platelets

reaction [16, 26]. Large charge/discharge voltage hysteresis is obviously observed between charge and discharge curves, which may result from a heterogeneous reaction mechanism of lithium insertion and extraction [6, 16, 26]. The first specific lithiation capacity is 841 mAh g^{-1} for CoO/CNF composite and 1091 mAh g^{-1} for CoO platelet respectively. The coulombic efficiencies for CoO/CNF composites and CoO platelets rapidly rise from 77.9% and 70.1% in the first cycle to 97% and 90% in the second onem respectively, and then an efficiency of mostly above 98% is maintained in the following cycles for both the samples. Even after 100 cycles, the reversible capacity of the CoO/CNF composite electrode is still kept at 725.8 mAh g^{-1} (Fig. 5b). On the contrary, the capacity declines rapidly during initial cycling for CoO platelets without CNF, but its following cycles remain stable and its specific capacity is lower than that of CoO/CNF composites. The CoO/CNF composites show larger capacity and better charge and discharge performance than the corresponding CoO platelets. Furthermore, both CoO platelets and CoO/CNF composites show better capacity retention and cycle-ability than the previous reported CoO electrode materials [2, 9].

The more remarkable advantage of this composite material is the high-rate capability. Fig. 6a shows the influence of the change of charge rates on the capacity retention. The cell was discharged at 0.2 C to ensure initial conditions for each charge, and charge rates were ranged from 0.2 C to 10 C at 25 °C. With the enhanced current rate, the capacity decreases regularly. When the charge rates are≥ 4 C, the reversible capacity decreases from 400 mAh g^{-1} at 4 C to 250 mAh g^{-1} at 10 C. Interestingly, while the charge rates are ≤2 C, especially at 2 C, the composite material remains rather high reversible capacity about 600 mAh g^{-1}. Furthermore, the capacity can be completely recovered when the discharge rate returns to 0.2 C rate, indicating that CoO/CNF composite has good electrochemical reversibility and structural integrity.

The CoO/CNF composite material can not only supply large capacity under high-rate conditions, but also maintain good cycling stability. Figure 6b shows the charge capacities of the first 50 cycles for the composite electrodes

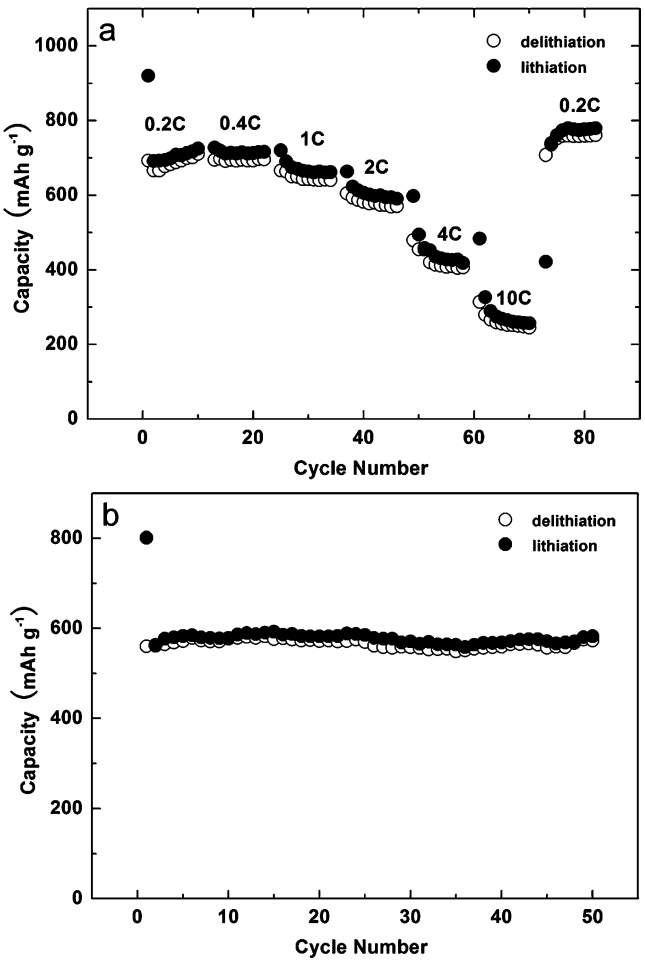

Fig. 6 **a** Reversible capacities during continuous cycling at various charge rates, **b** capacity-cycle number curve of CoO/CNF composites at 2 C

at higher rate of 2 C. After 50 cycles, the CoO composite electrodes still keep a rather high specific capacity of 580 mAh g^{-1}, which is about two times larger than that of CoO platelet (300 mAh g^{-1} at 2 C not showed here). In particular, the capacity does not tend to decline after 50 cycles. The high rate capability and corresponding capacities of CoO platelets are remarkably improved by adding 25.1 wt% CNFs. Thus, a strong synergistic effect of porous CoO platelets and conducting CNFs on their electrochemical performance is clearly observed during the charge/discharge process. Therefore, the CoO/CNF composites can be further developed for optimal performance as anode materials for high-energy LIBs in further search.

According to the results presented above, the significantly improved rate capability and cycle-ability of the CoO/CNF composite electrodes may attribute to the remarkable synergistic effect of the combination of porous structural stability and excellent conductivity through CNF connection. First, the CoO platelets are mainly composed of appropriate porous structure with average mesopore sizes of 30 nm. The porosity not only can enhance the electrolyte/CoO contact area and shorten the Li^+ ion diffusion length in the CoO platelet, but accommodate the mechanical stress induced by the volume change during the electrochemical reaction. Second, the CoO/CNF composite with entangled and branched bundles of CNF can produce a higher electronic conductivity than the single CoO platelet. Third, according to CVs analysis of the CoO/CNF composite electrode, an effective and stable SEI can be formed on the electrode surface, which ensures the structural stability and integrity of the composite electrode over many charge-discharge cycles. These features are particularly helpful for high power applications when the battery is charge or discharged at high current. As a result, due to their unique composite architecture with appropriate porosity, good electronic and ion conductivity, the CoO/CNF composites can achieve a good cycle-ability and high rate capability.

Conclusions

In summary, novel platelike CoO/CNF composite has been prepared by means of simple thermal decomposition of β-$Co(OH)_2$/CNF precursor, which can be synthesized on a large scale by a surfactant-free hydrothermal method. When evaluated as electrode materials for LIBs, the as-prepared platelike CoO/CNF composites exhibit superior Li-battery performance with high capacity, good cycle life and high rate capability (delivering a stable specific capacity of 580 mAh g^{-1} at 2 C after 50 cycles), which is mainly due to their appropriate porosity, short and facile diffusion paths, good electronic and ion conductivity, and structural stability during discharge/charge cycles. Considering the outstanding performance and cost-effective synthesis, we believe as-prepared platelike CoO/CNF composite could be a promising alternative negative electrode material for high-energy rechargeable LIBs.

Acknowledgements The authors thank Prof. Jun Yang and Prof. Yanna Nuli (Shanghai Jiao Tong University) for their help with the electrochemical experiments and results discussion.

References

1. Dahn JR, Zheng T, Liu Y, Xue JS (1995) Science 270:590–593
2. Poizot P, Laruelle S, Grugeon S, Dupont L, Tarascon JM (2000) Nature 407:496–499
3. Derrien G, Hassoun J, Panero S, Scrosati B (2007) Adv Mater 19:2336–2340
4. Xiang JY, Tu JP, Huang XH, Yang YZ (2008) J Solid State Electrochem 12:941–945
5. Pan Q, Liu J (2009) J Solid State Electrochem 13:1591–1597
6. Yu Y, Chen CH, Shui JL, Xie S (2005) Angew Chem Int Ed 44:7085–7089
7. Li WY, Xu LN, Chen J (2005) Adv Funct Mater 15:851–857
8. Do JS, Weng CH (2005) J Power Sources 146:482–486
9. Wang GX, Chen Y, Konstantinov K, Lindsay M, Liu HK, Dou SX (2002) J Power Source 109:142–147
10. Lou XW, Deng D, Lee JY, Feng J, Archer LA (2008) Adv Mater 20:258–262
11. Yao W, Yang J, Wang J, Nuli Y (2008) J Electrochem Soc 155: A903–A908
12. Grugeon S, Laruelle S, Dupont L, Tarascon JM (2003) Solid State Sci 5:895–904
13. Li Y, Tan B, Wu Y (2008) Nano Lett 8:265–270
14. Lu Y, Wang Y, Zou Y, Jiao Z, Zhao B, He Y, Wu M (2010) Electrochem Commun 12:101–105
15. Liu D, Garcia BB, Zhang Q, Guo Q, Zhang Y, Sepehri S, Cao G (2009) Adv Funct Mater 19:1015–1023
16. Poizot P, Laruelle S, Grugeon S, Tarascon JM (2002) J Electrochem Soc 149:A1212–A1217
17. Dollé M, Poizot P, Dupont L, Tarascon JM (2002) Electrochem Solid-State Lett 5:A18–A21
18. Dedryvère R, Laruelle S, Grugeon S, Poizot P, Gonbeau D, Tarascon JM (2004) Chem Mater 16:1056–1061
19. Lee JK, An KW, Jub JB, Cho BW, Cho WI, Park D, Yun KS (2001) Carbon 39:1299–1305
20. Subramanian V, Zhu H, Wei B (2006) J Phys Chem B 110:7178–7183
21. Wolf H, Pajkic Z, Gerdes T, Willert-Porada M (2009) J Power Sources 19:157–161
22. Kim C, Yang KS, Kojima M, Yoshida K, Kim YJ, Kim YA, Endo M (2006) Adv Funct Mater 16:2393–2397
23. Yao W, Yang J, Wang J, Tao L (2008) Electrochem Acta 53:7326–7330
24. Laruelle S, Grugeon S, Poizot P, Dollé M, Dupont L, Tarascon JM (2002) J Electrochem Soc 149:A627–A634
25. Do JS, Weng CH (2006) J Power Sources 159:323–327
26. Li H, Balaya P, Maier J (2004) J Electrochem Soc 151:A1878–A1885